Enhancement of the Efficacy of an Antagonist of an Extracellular Receptor by Attachment to the Surface of a Biocompatible Carrier

Charles A. Wartchow,[1] Susan E. Alters,[1] Pamela D. Garzone,[1] Lingyun Li,[1] Steven Choi,[1] Neal E. DeChene,[1] Tina Doede,[1] Linong Huang,[1] John S. Pease,[1] Zhimin Shen,[1] Susan J. Knox,[2] and Jeffrey L. Cleland[1,3,4]

Received January 25, 2004; accepted June 6, 2004

Purpose. In order to improve the *in vitro* and *in vivo* efficacy of an integrin antagonist (IA) of the extracellular domain of the αvβ3 integrin, a receptor upregulated on tumor neovasculature, the IA was attached to the surface of a dextran-coated liposome (DCL). IA-DCLs were characterized *in vitro*, and the pharmacokinetic and anti-tumor properties were assessed *in vivo*.

Methods. The *in vitro* binding properties were measured with purified integrin, endothelial cells, and melanoma cells. The pharmacokinetic parameters were measured in healthy mice with ^{14}C-labeled IA-DCLs and anti-tumor efficacy was assessed with the M21 human melanoma xenograft mouse model.

Results. *In vitro*, IC_{50} values for IA-DCLs and IA are similar, and IA-DCLs inhibit cell proliferation relative to controls. IA-DCLs are stable in serum, and the pharmacokinetic half-life in mice is 23 h. In the M21/mouse model, statistically significant inhibition of tumor growth was observed for mice treated with IA-DCLs, whereas controls including saline, DCLs lacking IA, and cyclo(RGDfV) were ineffective. Increased apoptosis and a reduction in vessel counts relative to controls were present in tumors from animals treated with IA-DCLs.

Conclusions. These results demonstrate that IA-DCLs are potent anti-angiogenic therapeutic agents with superior *in vivo* activity and pharmacology compared to unmodified IA.

KEY WORDS: angiogenesis; drug delivery; integrin; liposome; solid tumor.

INTRODUCTION

The αvβ3 integrin, a cell-surface receptor that binds to extracellular matrix proteins, has been implicated in diseases including cancer, diabetic retinopathy, macular degeneration, and inflammation (1). In cancer, the $\alpha_v\beta_3$ integrin is a promising therapeutic target because it is upregulated on tumor cells and endothelial cells that comprise tumor neovasculature, and $\alpha_v\beta_3$ is expressed at lower levels on normal vasculature (2–4). Additionally, this integrin is upregulated during angiogenesis and is likely involved in tumor cell proliferation, migration, and metastasis (5). Disruption of extracellular interactions with natural ligands by antagonists results in apoptosis. Peptide-based and peptidomimetic therapeutic agents based on the Arg-Gly-Asp (RGD) sequence are efficacious *in vitro* and in animal models (6,7), but utility is often limited by proteolysis *in vivo*, and rapid systemic clearance. RGD peptide- and peptidomimetic-liposome conjugates show efficacy *in vitro* and *in vivo*, but their clinical potential may be limited by a lack of specificity, which was not examined in these studies (8–10).

The delivery of a drug by encapsulation in a carrier often improves efficacy *in vivo* by increasing the pharmacokinetic (PK) half-life (11). However, this method is non-trivial; encapsulation efficiencies, release of the drug, and colloidal properties of the resulting formulation are highly dependent on the physical properties of the drug and the encapsulating materials. Biocompatible materials such as dextran have also been used as carriers, but these materials are cleared rapidly *in vivo* (12).

In order to overcome these limitations, we report the preparation of a dextran-coated liposome (DCL), a carrier for the covalent attachment of therapeutic agents to the surface, and its use for the enhancement of anti-tumor activity of a synthetic αvβ3 integrin antagonist (IA) that is non-efficacious *in vivo*. This IA binds selectively to the αvβ3 integrin, is 137-fold and 42-fold less potent against integrins αvβ5 and αIIbβIII, and binds to angiogenic, tumor-associated blood vessels *in vivo* (13). Covalent attachment of this agent to the surface of DCLs eliminates the need for extensive formulation efforts focused on optimizing encapsulation efficiency, and optimization of release rates that affect PK half-life and efficacy.

MATERIALS AND METHODS

General

Lipids were obtained from Avanti Polar Lipids (Alabaster, AZ). Cholesterol and trinitrobenzenesulfonic acid (TNBS) were obtained from the Sigma Chemical Company (St. Louis, MO) and Pierce (Rockford, IL), respectively. ^{14}C-DPPC was from American Radiolabeled Chemicals, Inc. (St. Louis, MO). $\alpha_v\beta_3$ integrin and vitronectin were obtained from Chemicon (Temecula, CA). Commercial 40 kD aminodextran, which was used to prepare DCLs for *in vivo* studies, was obtained from Molecular Probes (Eugene, OR). The NMR spectra of this material was identical to aminodextran prepared as described below. Reagents for the preparation and characterization of aminodextran were obtained from the Sigma/Aldrich/Fluka Chemical Company (St. Louis, MO). $\alpha_v\beta_3$ integrin antagonist (IA) was prepared as described previously (13). Liposome size was determined by dynamic light scattering (Brookhaven Instruments, Holtsville, NY).

Preparation of Aminodextran

Aminodextran was prepared as described previously (14). This method generates a 3-amino-2-hydroxypropyl ether

[1] Targesome Inc., Palo Alto, California, 94303, USA.
[2] Department of Radiation Oncology, Stanford University Medical Center, Stanford, California, 94305, USA.
[3] Current address: Novacea, Inc., San Francisco, California 94080, USA.
[4] To whom correspondence should be addressed. (e-mail cleland@novacea.com)

ABBREVIATIONS: DCL, dextran-coated liposome; EDAC, 1-ethyl-3-(3-dimethylaminopropyl)carbodiimide; H&E, hematoxylin and eosin; HUVEC, human umbilical vein endothelial cells; IA, integrin antagonist; PEG, polyethylene glycol; RGDfV, Arg-Gly-Asp-(D)-Phe-Val; TNBS, Trinitrobenzene sulfonate; TUNEL, terminal deoxynucleotide transferase-mediated dUTP nick-end labeled; TVQT, tumor volume quadrupling time.

derivative of dextran through the reaction of epichlorohydrin in the presence of zinc tetrafluoroborate, followed by displacement of the chloride with ammonia. This aminodextran has approximately 20–25 amines per dextran chain as determined by the TNBS assay (15) using β-alanine as a standard, and chemical derivatizations of dextran were confirmed by proton NMR (300 MHz, Varian Instruments, Palo Alto, CA).

Preparation of Dextran-Coated Liposomes (DCLs)

Liposomes containing DPPE-succinate (DPPE-S), cholesterol (CH), and DPPC (5/40/55 mole percent) were prepared by lyophilization of a mixture of these components from *t*-butanol followed by hydration with water and homogenization. In a typical procedure, water (150 ml) was added to a lyophilized cake of 101, 1000, and 383 mg of DPPE-S, DPPC, and cholesterol, respectively. This mixture was homogenized with a Microfluidics homogenizer at 16,000 psi. Alternatively, liposomes were prepared by adding a solution of DPPE-S (101 mg), DPPC (1000 mg) and cholesterol (383 mg) in *t*-butanol (30 ml) to water (300 ml), and *t*-butanol was removed by tangential flow filtration (TFF). The liposomes (1500 mg in 150 ml water) were added to aminodextran (1800 mg in 18 ml water) followed by 1 M EDAC (1.68 ml). Remaining succinate groups from unreacted DPPE-succinate were converted to amides by adding 2.5 M ammonium sulfate (0.68 ml) followed by 1 M EDAC (1.7 ml). After purification by TFF, the dextran content was determined to be 20–30 weight percent using the anthrone assay (16). Next, amino groups were succinylated with succinic anhydride (1 M, 1.2 ml DMSO), which was added to dextran-coated liposomes (1500 mg in 38 ml water) while maintaining the pH at 7 by adding 1 M NaOH. The succinamidodextran-liposome conjugates were purified by TFF. IA was attached to the liposomes (1500 mg in 75 ml water) by adding IA (150 mg in 3 ml DI water) and 1 M EDAC (1.6 ml). After purification by TFF, the IA-DCLs were 110 nm with a 5–95% Guassian distribution of 50–245 nm and a polydispersity of 3.8. IA loading was monitored by size exclusion chromatography with a Pharmacia HR 10/30 column with Sepharose CL-4B resin.

Potency Assay

IC_{50} values were determined with $\alpha_v\beta_3$ integrin-coated 96-well plates in a competition assay with a biotin-vitronectin conjugate (17). IA-DCLs and biotin-vitronectin conjugate were incubated with $\alpha_v\beta_3$ integrin-coated plates blocked with BSA, the plates were washed, streptavidin-HRP conjugate was added, LumiGlo chemiluminescent substrate was added, and signal was measured with a Wallac Victor plate reader.

Cell Adhesion Assay

The inhibition of cell adhesion was performed as described previously (18).

Inhibition of Cell Proliferation

Cell proliferation was assessed *in vitro* by incubating IA, IA-DCLs, or DCLs with human umbilical vein endothelial cells (HUVECs) at 80% confluence for 24 h, replacing the growth media, and measuring cell density at 72 h. Viable cells were measured with MTT, which is selectively converted by live cells, as described previously (19).

Determination of Pharmacokinetic Parameters and Biodistribution

IA-DCLs and DCLs labeled with ^{14}C-DPPC were administered intravenously to five nu/nu mice per time point at DCL doses of 150 mg/kg and 1 μCi per mouse. At each time point, the mice were sacrificed, and tissue samples or plasma was obtained. For each time point, tissue or plasma was pooled, and ^{14}C was measured using a scintillation counter. PK parameters were obtained using non-compartmental analysis of the data with the Winnlin application (version 4.0).

Tumor Growth Inhibition *in Vivo*

The M21 melanoma model was prepared by subcutaneous, dorsal injection of tumor cells into nude mice and all protocols were approved and performed in accordance with the ethical standards of the Stanford University animal facility. Mice with tumors ranging from 44-225 mm^3 were randomly assigned to treatment groups and received four doses of placebo or therapeutic agent by intravenous injection on days 0, 2, 4, and 6. Doses were 15 mg/kg each dose (60 mg/kg total) for IA-DCLs, IA, or cyclic peptide. Doses for DCLs were approximately 300 mg/kg (1200 mg/kg total). Tumor volume was measured three times per week until the tumors had quadrupled in size. Normalized tumor volumes were computed as tumor volume on the last day all animals were alive (day 13) divide by the tumor volume on the day of treatment initiation (day 0) and was computed separately for each individual animal. p values were obtained using Tukey's W procedure with normalized tumor volumes at 13 days post treatment as well as for tumor volume quadrupling times.

H&E Staining

Tumor sections were cut at 5 μm and fixed in methanol for 1 min. The slides were stained in hematoxylin for 1 min and rinsed in water for 2 min. After a quick dip in 2% ammonia water and rinse in water for 2 min, the slides were stained in eosin for 1 min. The slides were then dehydrated through graded ethanols, cleared in xylenes, and mounted in synthetic mounting media.

TUNEL Assay

TdT-mediated dUTP nick-end labeling (TUNEL) assays were performed to detect tumor apoptosis. Tumor samples were obtained and kept frozen in a –80°C freezer until 10 μm cryostat sections were cut at three different levels between the two poles of each tumor. The Tumor TACs kit from R&D Systems Inc. (Minneapolis, MN) was used for analysis of apoptosis. Tumor samples were fixed with 3.7% formaldehyde and the cell membranes were permeabilized with Cytonin reagent. DNA strand breaks were labeled with biotinylated nucleotides in Terminal deoxynucleotidyl Transferase (TdT) incubation buffer at 37°C for one hour. Apoptotic cells were visualized with brown precipitates generated by streptavidin-conjugated HRP in the presence of diaminobenzidine (DAB). Samples were counterstained with 1% methyl green to show viable cells.

Anti-CD31 Staining

Anti-CD31 staining was used to detect the tumor vasculature. Tumor samples were obtained and kept frozen in a

–80°C freezer until 10 μm cryostat sections were cut. Samples were air-dried for 2 h at room temperature and fixed in cold acetone for 5 min. The slides were then incubated with anti-CD31 primary antibody (BD Biosciences, Palo Alto, CA) for 1 h at room temperature followed by incubation with secondary biotinylated antibody for 30 min. Tumor vascular endothelial cells were visualized with brown precipitates generated by streptavidin-conjugated HRP in the presence of DAB.

RESULTS

IA-DCLs (Fig. 1) are prepared by using EDAC to covalently attach aminodextran to surface carboxyl groups of DPPE-succinate in 60 nm liposomes containing DPPE-succinate to generate an amide bond. The other components of the liposomes are DPPC, which is used in an FDA-approved liposomal formulation of amphotericin B (20), and cholesterol, which stabilizes lipid bilayers (21). Remaining unreacted amines on the aminodextran are converted to carboxylic acid groups by reaction with succinic anhydride, and the αvβ3 integrin antagonist, which contains a primary amine linker, is attached to the succinamidodextran on the surface of DCLs with EDAC. The resulting 110 nm IA-DCLs contain approximately 50 μg of IA per mg of dry vesicle, which corresponds to approximately 3,500 IA molecules per DCL based on geometric calculations (22). The increase in size from 60 nm for the liposome to 110 nm for the IA-DCL is a result of the thickness of the dextran coat, and attachment of the IA has a minimal effect on size. For comparison, attempts to prepare integrin-targeted liposomes without dextran resulted in lower drug loading, and a lower *in vitro* potency (data not shown).

IA-DCLs Bind to Cellular and Purified αvβ3 Integrin *in Vitro*

In a competition assay, IA-DCLs have an IC_{50} of 52 ± 8 nM for the inhibition of the binding of biotinylated vitronectin to purified human αvβ3 integrin. In comparison, free IA has an IC_{50} of 19 ± 5 nM. IA-DCLs also inhibit the binding of human umbilical vein endothelial cells (HUVECs), human microvascular endothelial cells (HMVECs), M21 human melanoma cells, and mouse endothelial cells to vitronectin with IC_{50} values of 0.3–3.5 μM, where IA has IC_{50} values of 0.3–2.7 μM (Table I) and DCLs lacking IA did not inhibit binding at concentrations in the range of the IC_{50} values. Furthermore, IA-DCLs reproducibly inhibit the proliferation of HUVECs *in vitro* at micromolar concentrations, whereas IA alone had a more limited effect, and DCLs lacking IA had no effect. For example, after a 72-h incubation in the presence of IA-DCLs containing IA at 1.6 μM, viable cell density was 60 ± 5%, compared to 100 ± 3% for untreated cells. Cells treated with identical concentrations of IA or DCLs lacking IA yielded cell densities of 75 ± 6% and 98 ± 1%, respectively.

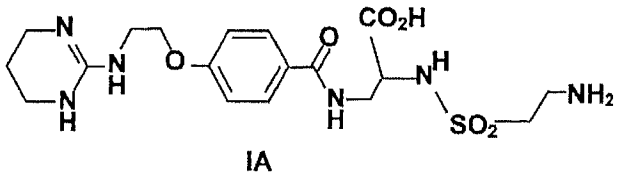

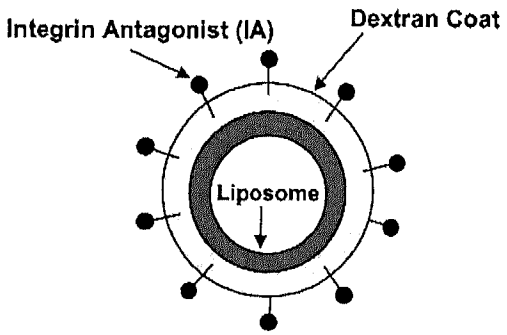

Fig. 1. Structure of integrin antagonist and representation of an IA-DCL.

IA-DCLs Are Stable in Serum

The stability of drug-carrier conjugates in serum is paramount for obtaining efficacy *in vivo*, and IA-DCLs are stable in 90% mouse serum *in vitro*. Stability in serum was assessed by incubating samples at 37°C, separating the IA-DCL from serum components by size exclusion chromatography and measuring retained potency. At 24 h, IA-DCLs retained 44.5 ± 3.5% of the original potency in the competition assay with biotinylated vitronectin. With respect to the integrity of the particle in serum, IA-DCLs and DCLs lacking IA prepared with ^{14}C-labeled DPPC retain 79% of this label at 48 h as determined by size exclusion chromatography and measurement of ^{14}C in the fractions containing DCLs.

IA-DCLs Have a Long Half-life and a Restricted Volume of Distribution in Healthy Mice

The pharmacokinetic parameters and biodistribution of IA-DCLs and DCLs were determined with materials containing DPPC labeled at the ester with ^{14}C. For this study, the size, dextran content, and IA loading of these particles were representative of those used for *in vivo* efficacy studies. The materials were administered to healthy nu/nu mice (n = 5) by intravenous injection at doses of 150 mg/kg DCL or IA-DCL, and 7.5 mg/kg IA for IA-DCL.

The IA-DCLs and DCLs have comparable pharmacokinetics and biodistribution (Table II). The elimination half-life ($t_{1/2\beta}$) is 23 h and 18 h for IA-DCLs and DCLs lacking IA, respectively. The biodistribution of IA-DCLs and DCLs in this study is also similar, with the exception of plasma and

Table I. IC_{50} Values for the Inhibition of the *in Vitro* Binding of Endothelial and Tumor Cells to Vitronectin[a]

Agent	IC_{50} ± SD (μM)			
	MS1 EC	HUVEC	HMVEC	M21
IA	0.31 ± 0.02	2.7 ± 0.4	0.78 ± 0.2	0.29 ± 0.4
IA-DCL	1.5 ± 0.3	1.4 ± 0.1	3.5 ± 0.3	0.27 ± 0.4
Cyclo(RGDfV)	0.98 ± 0.1	2.4 ± 0.3	0.74 ± 0.1	ND

Abbreviations: HMVEC, human microvascular endothelial cells; HUVEC, human umbilical vein endothelial cells; M21, M21 human melanoma cells; MS1 EC, mouse endothelial cells; SD, standard deviation.

[a] At identical DCL concentrations, control DCLs did not inhibit the binding of HMVECs, HUVECs or MS1 ECs.

Table II. Pharmacokinetic Parameters of ^{14}C-Labeled IA-DCLs and DCLs Lacking IA Following Intravenous Injection in nu/nu Mice

PK parameter	IA-DCL	DCL
Cmax (cpm/gm)	7.1×10^6	9.4×10^6
Tmax (h)	0.5	2.0
$AUC_{0-48\ h}$ (cpm · ml^{-1} · h)	2.3×10^7	4.4×10^7
AUC_{INF} (cpm · ml^{-1} · h)	2.4×10^7	4.5×10^7
Elimination half-life $t_{1/2\beta}$ (h)	23	18

Abbreviations: AUC, area under curve; cpm, counts per minute.

lymph accumulation (Fig. 2). The primary site of accumulation, determined by comparing relative AUC values for the duration of this study ($AUC_{0-48\ h}$), is the plasma compartment, suggesting vascular confinement. Other significant sites of accumulation were the liver, spleen, and lymph (6–25%), which are RES components. With respect to the RES components, an increase of ~5–7% accumulation was observed for IA-DCLs relative to DCLs lacking IA, and accumulation in the lymph was ~4% lower for IA-DCLs relative to DCLs lacking IA. Minimal accumulation was observed in the heart, lung, muscle, and kidney (<4%). Plasma and lymph distribution were ≈2- and 3-fold lower for IA-DCLs relative to DCLs.

IA-DCLs Are Effective Anti-tumor Agents *in Vivo*

To test the hypothesis that presentation of the IA on the surface of a carrier would improve efficacy, IA-DCLs (15 mg/kg IA, ~300 mg/kg DCL), IA, DCLs lacking IA, and saline were administered intravenously on days 0, 2, 4, and 6 to female nu/nu mice with established human M21 melanoma tumors in the range of 44–225 mm^3 with a mean of ~100 mm^3 for each group. No significant changes in body weight were observed during treatment. Significant differences in normalized tumor volumes were observed for IA-DCLs in the M21 human melanoma model when compared to buffer, and matching doses of DCL lacking IA and IA alone (ANOVA, $n = 9$, day 11, Tukey's W procedure, $p < 0.008$). The rate of tumor growth was assessed by comparisons of tumor volume quadrupling times (TVQTs) indicating significant differences for IA-DCLs (26.3 ± 14 days) relative to IA (12.0 ± 3.7 days), DCLs lacking IA (9.3 ± 2.6 days), and saline (8.7 ± 2.1 days). These results demonstrated the superior efficacy of treatments with IA-DCLs compared to IA at the same drug dose.

In a confirming study, IA-DCLs were again superior therapeutic agents relative to controls including DCLs alone, saline, and a control cyclic peptide, cyclo(RGDfV). Statistically significant differences in normalized tumor volumes were observed for IA-DCLs in the same M21 human melanoma model at IA and DCL doses of 15 mg/kg and ~1200 mg/kg, respectively, when compared to saline, and matching doses of DCLs lacking IA (ANOVA, $n = 8$, day 13, Tukey's W procedure, $p < 0.05$). Comparisons of TVQTs indicated statistically significant differences between tumors treated with IA-DCLs (23.0 ± 8.8 days) and saline (11.7 ± 2.2 days) or DCLs alone (11.9 ± 2.6 days). Significant inhibition of tumor growth was not observed for cyclo(RGDfV). These data are summarized in Fig. 3.

Ex vivo Analysis of Tumor Sections Shows That IA-DCLs Are Anti-angiogenic Agents

H&E, TUNEL, and CD31 staining of serial tumor sections from tumors excised 24 h after the final treatment confirm that IA-DCLs had a significant impact on tumor physiology (Fig. 4). Tumors that were treated with IA-DCLs exhibit significant areas of necrosis relative to controls treated with saline, as shown by H&E staining. Furthermore, TUNEL staining revealed that necrosis is a result of apoptosis. Vessel counts determined in tumors treated with IA-DCLs were 40% lower relative to the control treated with saline, which is consistent with an anti-angiogenic mechanism of action. Necrosis and apoptosis was minimal in tumors treated with IA, and vessel counts were similar to those in tumors treated with saline.

DISCUSSION

These results demonstrate that the *in vivo* efficacy of a nonefficacious small molecule integrin antagonist against the extracellular domain of a receptor is significantly improved by presentation on the surface of a biocompatible, nanoscale carrier. The carrier, a dextran-coated liposome, consists of biocompatible materials including phospholipids, and dextran, which is clinically approved for use as a plasma ex-

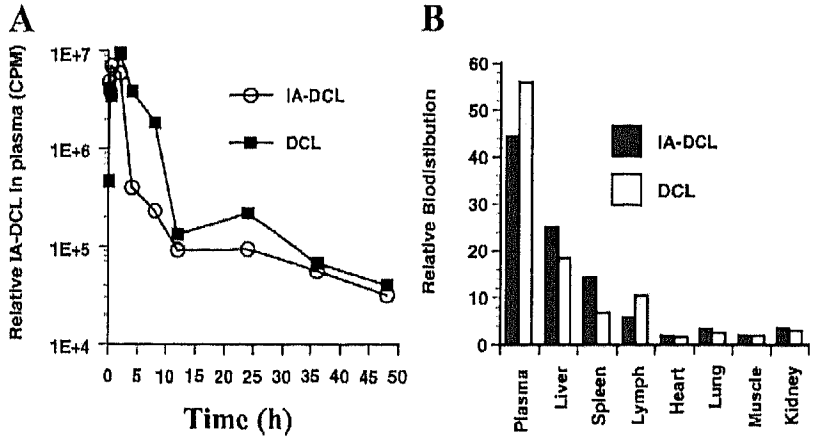

Fig. 2. (A) Plasma clearance of ^{14}C-labeled IA-DCLs and DCLs lacking IA in nu/nu mice. (B) Biodistribution of IA-DCLs and DCLs in healthy mice at 24 h. For these studies, IA-DCL and DCL were injected intravenously and plasma or tissue samples were pooled. The standard deviation was less than 10% for repeat measurements of a given sample.

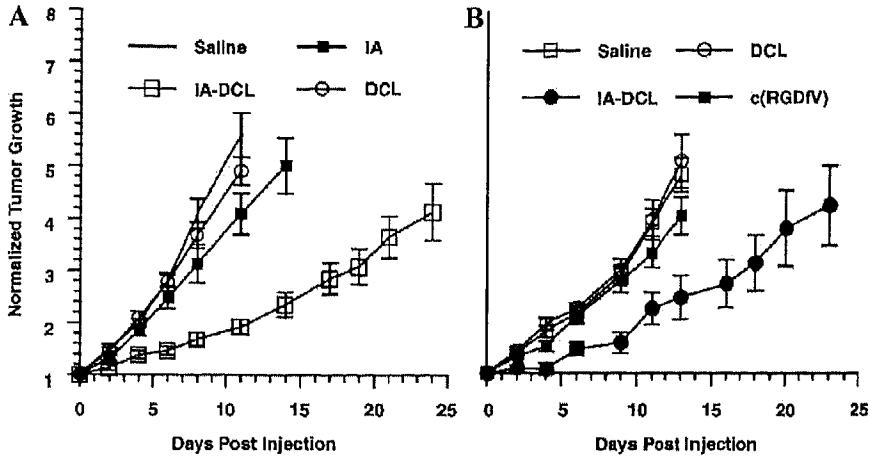

Fig. 3. Inhibition of tumor growth by IA-DCLs in the M21 melanoma model in nu/nu mice. (A) Comparison of IA-DCLs, IA alone, DCLs alone, and saline. (B) Additional experiment comparing control peptide cyclo(RGDfV) with IA-DCLs, DCLs, and saline. In both experiments, animals were dosed intravenously on days 0, 2, 4, and 6. Drug dose for IA, IA-DCLs, and cyclo(RGDfV) was 15 mg/kg for each dose, and the DCL dose was equivalent to the DCL exposure in the IA-DCL groups. Normalized tumor volumes were calculated from measurements of subcutaneous, dorsal tumor cell implants as described in "Materials and Methods."

pander. Furthermore, IA-DCLs have additional desirable features including selectivity for the αvβ3 integrin, which is expressed on tumor cells and tumor-associated endothelial cells, and it is expressed in low levels in normal vasculature (2–4). Other relevant features include recognition of cellular αvβ3 integrin *in vitro*, stability in serum *in vitro*, a favorable PK half-life, and favorable biodistribution *in vivo*. Because the antagonist is selective for the αvβ3 integrin, toxicity associated with targeting similar receptors in healthy tissue including integrin αvβ5, which also contains the αv subunit, and integrin αIIbβIII, which is expressed on platelets (23), may be limited.

IA-DCLs have superior pharmacological characteristics including vascular confinement and a prolonged half-life. The elimination half-life of DCLs is comparable to the half-life for liposomes that contain polyethylene glycol (PEG) lipids, which have a longer half-life than traditional liposomes (22,24). However, ~1% of the injected dose remains after 48 hrs, whereas levels of PEG liposomes are markedly higher for a similar time period (22). A commercial stealth liposome formulation of doxorubicin (Doxil) that contains PEG lipids is currently dosed every 2–3 weeks in humans, suggesting that similar dosing regimens may be useful for DCLs. The IA-DCLs and DCLs are distributed primarily in the plasma compartment with minimal uptake in organs such as the heart, lung, and kidney. The observed biodistribution is a significant advantage for therapeutic agents that are targeted to vascular receptors such as endothelial cells (IA-DCLs) and diseased blood cells. Additionally, confining the drug to the plasma compartment may potentially minimize systemic organ toxicity.

In vivo, IA-DCLs effectively inhibit the growth of tumors in the M21 nu/nu mouse melanoma model in two sepa-

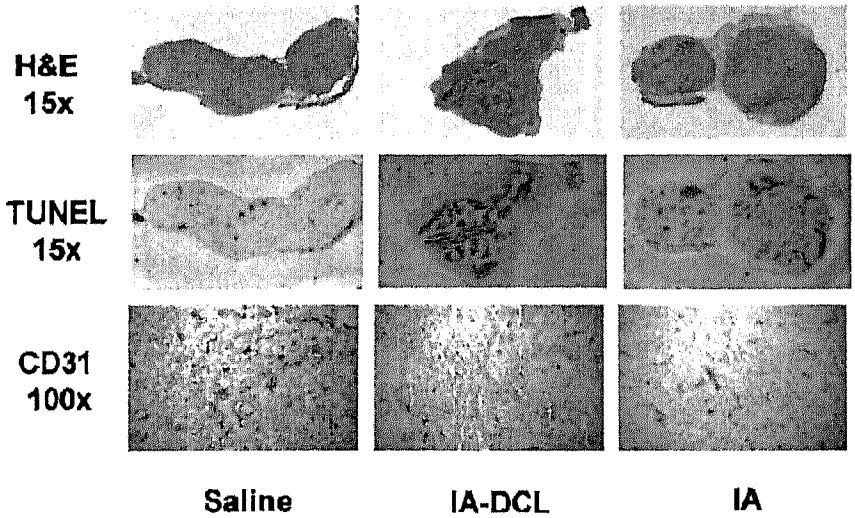

Fig. 4. Histologic analysis including H&E, TUNEL, and CD31 staining of serial sections of tumors treated with IA-DCLs, and IA.

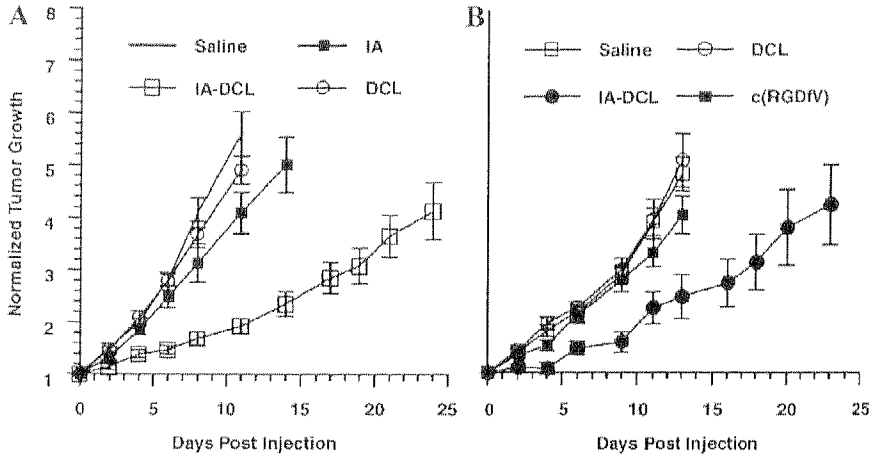

Fig. 3. Inhibition of tumor growth by IA-DCLs in the M21 melanoma model in nu/nu mice. (A) Comparison of IA-DCLs, IA alone, DCLs alone, and saline. (B) Additional experiment comparing control peptide cyclo(RGDfV) with IA-DCLs, DCLs, and saline. In both experiments, animals were dosed intravenously on days 0, 2, 4, and 6. Drug dose for IA, IA-DCLs, and cyclo(RGDfV) was 15 mg/kg for each dose, and the DCL dose was equivalent to the DCL exposure in the IA-DCL groups. Normalized tumor volumes were calculated from measurements of subcutaneous, dorsal tumor cell implants as described in "Materials and Methods."

pander. Furthermore, IA-DCLs have additional desirable features including selectivity for the αvβ3 integrin, which is expressed on tumor cells and tumor-associated endothelial cells, and it is expressed in low levels in normal vasculature (2–4). Other relevant features include recognition of cellular αvβ3 integrin *in vitro*, stability in serum *in vitro*, a favorable PK half-life, and favorable biodistribution *in vivo*. Because the antagonist is selective for the αvβ3 integrin, toxicity associated with targeting similar receptors in healthy tissue including integrin αvβ5, which also contains the αv subunit, and integrin αIIbβIII, which is expressed on platelets (23), may be limited.

IA-DCLs have superior pharmacological characteristics including vascular confinement and a prolonged half-life. The elimination half-life of DCLs is comparable to the half-life for liposomes that contain polyethylene glycol (PEG) lipids, which have a longer half-life than traditional liposomes (22,24). However, ~1% of the injected dose remains after 48 hrs, whereas levels of PEG liposomes are markedly higher for a similar time period (22). A commercial stealth liposome formulation of doxorubicin (Doxil) that contains PEG lipids is currently dosed every 2–3 weeks in humans, suggesting that similar dosing regimens may be useful for DCLs. The IA-DCLs and DCLs are distributed primarily in the plasma compartment with minimal uptake in organs such as the heart, lung, and kidney. The observed biodistribution is a significant advantage for therapeutic agents that are targeted to vascular receptors such as endothelial cells (IA-DCLs) and diseased blood cells. Additionally, confining the drug to the plasma compartment may potentially minimize systemic organ toxicity.

In vivo, IA-DCLs effectively inhibit the growth of tumors in the M21 nu/nu mouse melanoma model in two sepa-

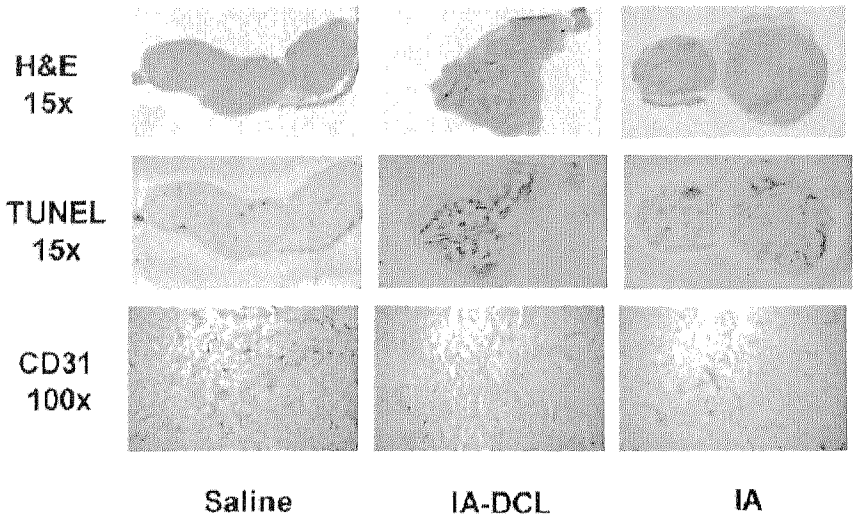

Fig. 4. Histologic analysis including H&E, TUNEL, and CD31 staining of serial sections of tumors treated with IA-DCLs, and IA.

rate studies, whereas DCLs lacking IA were ineffective. IA-DCLs were also superior therapeutic agents relative to IA and cyclo(RGDfV), which has been effective for the treatment of glioma, colon carcinoma, and melanoma in animal models (25–27). The lack of efficacy for cyclo(RGDfV) observed in the present study is likely due to the administration of very high and frequent doses that are required to achieve significant efficacy.

The histopathology observed for tumors treated with IA-DCLs is consistent with an anti-angiogenic mechanism and exhibits general necrosis by H&E staining, reduced vessel counts by CD31 staining, and apoptosis, which was determined by TUNEL staining. These observations are consistent with the binding of IA-DCLs to cells which express αvβ3 in the tumor which results in apoptosis through "outside-in" signaling of integrins. The apoptotic mechanism is believed to involve the disruption of signaling mediated by focal adhesion kinase (FAK), which interacts with the intracellular domain of the αvβ3 integrin in clusters called focal adhesions. This disruption results in the activation of caspase 8, which causes apoptosis (5). This effect is likely the result of the binding of IA-DCLs to tumor-associated endothelial cells, but may also be due, in part, to binding to nearby M21 melanoma cells that are accessible to the tumor vasculature, since M21 cells also express the αvβ3 integrin. Further access to tumor cells remote from the vasculature is unlikely, as the elimination half-life is consistent with vascular compartmentalization, and particles in the size range used for these studies are not known to penetrate solid tumors. In addition, results from a previous study using the same IA also support an anti-angiogenic mechanism as opposed to a direct effect on the tumor.

The inhibition of HUVEC proliferation *in vitro* is also consistent with an anti-angiogenic mechanism since IA-DCLs inhibit cell proliferation, while control IA has a more limited effect, and DCLs lacking IA have no effect. These data suggest that these agents may have anti-tumor properties in humans.

Overall, these studies have demonstrated the ability of a unique carrier system (DCLs) to enhance the efficacy and pharmacology of a small molecule anti-angiogenic compound (IA). This potent, selective anti-angiogenic therapeutic has several advantages over current anti-angiogenics such as its vascular confinement, long elimination half-life, and high potency due to the high drug density (≈3500 drug molecules per carrier).

ACKNOWLEDGMENTS

We thank Dr. Mary Tanga at SRI International, Menlo Park, CA, for leading the synthesis of integrin antagonist and Comparative Biosciences (Mountain View, CA) for performing the pharmacokinetics and biodistribution study. Additionally, we thank Targesome Inc. for funding these studies.

REFERENCES

1. J. C. Gutheil, T. N. Campbell, P. R. Pierce, J. D. Watkins, W. D. Huse, D. J. Bodkin, and D. A. Cheresh. Targeted antiangiogenic therapy for cancer using Vitaxin: a humanized monoclonal antibody to the integrin αvβ3. *Clin. Cancer Res.* **6**:3056–3061 (2000).
2. C. L. Gladson. Expression of integrin αvβ3 in small blood vessels of glioblastoma tumors. *J. Neuropathol. Exp. Neuro.* **55**:1143–1149 (1996).
3. R. Max, R. R. Gerritsen, P. T. Nooijen, S. L. Goodman, A. Sutter, U. Keilholz, D. J. Ruiter, and R. M. De Waal. Immunohistochemical analysis of integrin αvβ3 expression on tumor-associated vessels of human carcinomas. *Int. J. Cancer* **71**:320–324 (1997).
4. L. Bello, J. Zhang, D. C. Nikas, J. F. Strasser, R. M. Villani, D. A. Cheresh, R. S. Carroll, and P. M. Black. αvβ3 and αvβ5 integrin expression in meningiomas. *Neurosurgery* **47**:1185–1195 (2000).
5. J. D. Hood and D. A. Cheresh. Role of integrins in cell invasion and migration. *Nat. Rev. Cancer* **2**:91–100 (2002).
6. J. S. Kerr, A. M. Slee, and S. A. Mousa. Small molecule alpha v integrin antagonists: novel anticancer agents. *Expert Opin. Investig. Drugs* **9**:1271–1279 (2000).
7. J. S. Kerr, A. M. Slee, and S. A. Mousa. The alpha v integrin antagonists as novel anticancer agents: an update. *Expert Opin. Investig. Drugs* **11**:1765–1774 (2002).
8. N. Oku, Y. Tokudome, C. Koike, N. Nishikawa, H. Mori, I. Saiki, and S. Okada. Liposomal Arg-Gly-Asp analogs effectively inhibit metastatic B16 melanoma colonization in murine lungs. *Life Sci.* **58**:2263–2270 (1996).
9. K. Kurohane, Y. Namba, and N. Oku. Liposomes modified with a synthetic Arg-Gly-Asp mimetic inhibit lung metastasis of B16BL6 melanoma cells. *Life Sci.* **68**:273–281 (2000).
10. R. Schiffelers, G. Molema, T. L. ten Hagen, A. P. Janssen, A. J. Schraa, R. J. Kok, G. A. Koning, and G. Storm. Ligand-targeted liposomes directed against pathological vasculature. *J. Liposome Res.* **12**:129–135 (2002).
11. T. M. Allen. Liposomal drug formulations. Rationale for development and what we can expect for the future. *Drugs* **56**:747–756 (1998).
12. R. Mehvar. Dextrans for targeted and sustained delivery of therapeutic and imaging agents. *J. Control. Rel.* **69**:1–25 (2000).
13. J. D. Hood, M. Bednarski, R. Frausto, S. Guccione, R. A. Reisfeld, R. Xiang, and D. A. Cheresh. Tumor regression by targeted gene delivery to the neovasculature. *Science* **296**:2404–2407 (2002).
14. P. Hubert, J. Mester, E. Dellacherie, J. Neel, and E. E. Baulieu. Soluble biospecific macromolecule for purification of estrogen receptor. *Proc. Natl. Acad. Sci. USA* **75**:3143–3147 (1978).
15. A. F. Habeeb. Determination of free amino groups in proteins by trinitrobenzenesulfonic acid. *Anal. Biochem.* **14**:328–336 (1966).
16. T. A. Scott and E. H. Melvin. Determination of dextran with anthrone. *Anal. Chem.* **25**:1656–1661 (1953).
17. G. A. Sulyok, C. Gibson, S. L. Goodman, G. Holzemann, M. Wiesner, and H. Kessler. Solid-phase synthesis of a nonpeptide RGD mimetic library: new selective αvβ3 integrin antagonists. *J. Med. Chem.* **44**:1938–1950 (2001).
18. J. M. Wu, M. P. Rosser, A. R. Howlett, and R. I. Feldman. In A. Howlett (ed.), *Integrin Protocols*, Humana Press, Totowa, NJ, 1999 pp. 211–217.
19. R. D. Petty, L. A. Sutherland, E. M. Hunter, and I. A. Cree. Comparison of MTT and ATP-based assays for the measurement of viable cell number. *J. Biolumin. Chemilumin.* **10**:29–34 (1995).
20. I. M. Hann and H. G. Prentice. Lipid-based amphotericin B: a review of the last 10 years of use. *Int. J. Antimicrob. Agents* **17**:161–169 (2001).
21. H. M. Patel, N. S. Tuzel, and B. E. Ryman. Inhibitory effect of cholesterol on the uptake of liposomes by liver and spleen. *Biochim. Biophys. Acta* **761**:142–151 (1983).
22. D. L. Iden and T. M. Allen. In vitro and in vivo comparison of immunoliposomes made by conventional coupling techniques with those made by a new post-insertion approach. *Biochim. Biophys. Acta* **1513**:207–216 (2001).
23. B. S. Coller, K. Anderson, and H. F. Weisman. New antiplatelet agents: platelet GPIIb/IIIa antagonists. *Thromb. Haemost.* **74**: 302–308 (1995).
24. T. M. Allen and C. Hansen. Pharmacokinetics of stealth versus conventional liposomes: effect of dose. *Biochim. Biophys. Acta* **1068**:133–141 (1991).
25. S. Chatterjee, A. Matsumura, J. Schradermeier, and G. Y. Gillespie. Human malignant glioma therapy using anti-αvβ3 integrin agents. *J. Neurooncol.* **46**:135–144 (2000).
26. J. Haier, U. Goldmann, B. Hotz, N. Runkel, and U. Keilholz. Inhibition of tumor progression and neoangiogenesis using cyclic RGD- peptides in a chemically induced colon carcinoma in rats. *Clin. Exp. Metastasis* **19**:665–672 (2002).
27. R. Allman, P. Cowburn, and M. Mason. In vitro and in vivo effects of a cyclic peptide with affinity for the alpha v beta 3 integrin in human melanoma cells. *Eur. J. Cancer* **36**:410–422 (2000).